RC25101 (W1101-068) January 18, 2011
Other

IBM Research Report

Use of Mutant-Specific Ion Channel Characteristics for Risk Stratification of Long QT Syndrome Patients

Christian Jons[1], Jin O-Uchi[1], Arthur J. Moss[1], Matthias Reumann[2], John J. Rice[2], Ilan Goldenberg[2], Wojciech Zareba[1], Arthur A.M. Wilde[3], Wataru Shimizu[4], Jorgen K. Kanters[5], Scott McNitt[1], Nynke Hofman[3], Jennifer L. Robinson[1], Coeli M.B. Lopes[1]

[1]Department of Medicine
University of Rochester School of Medicine and Dentistry
New York, USA

[2]IBM Research Division
Thomas J. Watson Research Center
P.O. Box 218
Yorktown Heights, NY 10598 USA

[3]Academic Medical Centre
University of Amsterdam
Amsterdam, The Netherlands

[4]National Cardiovascular Center
Suita, Japan

[5]Gentofte University Hospital
and
The Danish National Research Foundation Center for Cardiac Arrhythmias
Copenhagen, Denmark

Research Division
Almaden - Austin - Beijing - Cambridge - Haifa - India - T. J. Watson - Tokyo - Zurich

Use of Mutant-Specific Ion Channel Characteristics for Risk Stratification of Long QT Syndrome Patients

Christian Jons[1]*, Jin O-Uchi[2]*, Arthur J. Moss[1], Matthias Reumann[3], John J. Rice[3], Ilan Goldenberg[3], Wojciech Zareba[1], Arthur A.M. Wilde[4], Wataru Shimizu[6], Jorgen K. Kanters[7, 8], Scott McNitt[1], Nynke Hofman[5], Jennifer L. Robinson[1] and Coeli M.B. Lopes[2]

* CJ and JO-U contributed equally to this work.

[1]Cardiology Division, Department of Medicine, University of Rochester School of Medicine and Dentistry, NY USA. [2] Aab Cardiovascular Research Institute, Department of Medicine, University of Rochester School of Medicine and Dentistry, NY USA. [3]Functional Genomics and Systems Biology Group, IBM T.J. Watson Research Center, NY USA. [4]Heart failure Research Centre, Department of Cardiology and [5]Department of Clinical Genetics , Academic Medical Centre, University of Amsterdam, Amsterdam, The Netherlands. [6]National Cardiovascular Center, Suita, Japan. [7]Gentofte University Hospital, Copenhagen, Denmark. [8]The Danish National Research Foundation Center for Cardiac Arrhythmias, Copenhagen, Denmark.

Corresponding Author:

Coeli M.B. Lopes

Cardiovascular Research Institute, Department of Medicine, University of Rochester, 601 Elmwood Ave, Box CVRI, Rochester, NY, 14642, USA. Phone: (585) 2769784, Fax: (585) 2759830. email: coeli_lopes@urmc.rochester.edu

ABSTRACT

Inherited Long QT syndrome (LQT) is caused by mutations in ion channels that delay cardiac repolarization, increasing the risk of sudden death from ventricular arrhythmias. Currently, the risk of sudden death in subjects with LQT is estimated from clinical parameters such as age, gender and the QT interval (QTc $\geq$ 500 ms). Even though a number of mutations can cause LQT, mutation-specific information is rarely used. LQT type 1 is one of the most common forms of LQT and is caused by mutations in the I_{Ks} channel α-subunit, KCNQ1. We investigated whether mutation-specific changes in IKs function can predict cardiac risk in LQT1. By correlating the clinical phenotype of 319 LQT type 1 patients with the cellular electrophysiological characteristics caused by an array of mutations in KCNQ1, we found that channels with a decreased rate of current activation are associated with increased risk of cardiac events (HR = 2.02), independent of the clinical parameters usually used for risk stratification. In patients with moderate QT prolongation (QTc < 500 ms), slower activation was an independent predictor for cardiac events (syncope, aborted cardiac arrest and sudden death) (HR = 2.10), whereas QT interval was not. Our results indicate that genotype and biophysical phenotype analysis may be useful for risk stratification of LQT1 patients and suggest that slow channel activation is associated with an increased risk of cardiac events.

Non-standard abbreviations and non-standard acronyms

LQTS: Long QT syndrome

LQT1: Long QT syndrome type 1

KCNQ1: IKs channel α-subunit

KCNE1: IKs channel β-subunit

QTc_m: median QTc prolongation

Tdp: Torsade de Point (Tdp)

EAD: early after depolarization

APD: action potential duration

HR: hazard ratio

INTRODUCTION

The slow potassium current (IKs) mediates cardiac repolarization. Mutations in the α-subunit, KCNQ1, of the IKs channel cause long QT syndrome type 1 (LQT1) (1). The identification of the gene responsible for this syndrome has allowed in-vitro characterization of mutation-related changes in the assembled channel. Current risk stratification of LQT1 subjects is performed mainly with clinical parameters such as age, gender and the QT interval; mutation-specific risk stratification is rarely used to guide therapy (2-5). Mutations with an autosomal dominant effect on channel function are associated with higher cardiac risk than those that impair channel function through haploinsufficiency (6). In addition, missense mutations and mutations in the transmembrane region of KCNQ1 are associated with a higher risk for cardiac arrhythmias(6). The mechanisms underlying these associations are unknown. Previous studies of a few mutations reported a poor correlation between decreased IKs current magnitude and the QTc interval in patients harboring the mutation (7-9). To date, no studies have attempted to correlate other channel characteristics to phenotype.

Recently, we showed that KCNQ1 mutations in highly conserved amino acids in the transmembrane region of human voltage-gated K^+ channels were associated with a high risk for cardiac events in the LQT1 subjects(10). Conserved amino acid residues are believed to control important aspects of channel function such as conduction and voltage gating of activation and deactivation(11, 12). Here we have set out: 1) to investigate the association of conventional measures of ion channel function (ion channel current magnitude, rate of current activation and deactivation, voltage dependence and maximal conductance) with QTc interval; 2) to determine whether ion-channel dysfunction contributes to the risk of cardiac events in LQT1 patients

independent of the standard phenotypic risk factors including QTc duration and 3) to investigate the mechanism underlying mutant-specific increase in cardiac risk, by evaluating electrophysiological parameters in the action potential of cardiomyocytes *in silico*.

RESULTS

Population and mutations characteristics

The clinical characteristics of the study patients are shown in Table 1. This population was drawn from the International Long QT Registry (see methods for details). All patients were genetically confirmed carriers of a single LQTS-causing mutation in the KCNQ1 gene and were enrolled over the past 20-30 years. Clinical follow-up data for these patients were used to relate altered cellular electrophysiology to cardiac risk. To be able to confidently estimate the mutation-specific clinical course and include as many different mutations as possible, we included only mutations involving 10 patients or more. A total of 17 mutations present in 387 LQT1 patients drawn from 4 LQTS international registries were included in the study. Most of the mutations were found in more than one family (59%), eight were found in two or more registries, 2 mutations were found in more than one family in the same registry and 7 mutations (41%) were found in just one family in one registry. QT prolongation among carriers of the same mutation is variable. To correlate conventional measures used for clinical risk stratification with functional cellular expression measurements, we calculated the median QTc prolongation in the carrier population (QTc_m) for each individual mutation. QTc_m was significantly prolonged for all but one mutation (D611Y). QTc is missing for 67 patients that died before QTc was evaluated. At least 9 patients were used to calculate the median QTc for each mutation studied.

Only missense mutations were used in this study because nonsense mutations are not expected to produce functional mutant channel subunits, and missense mutations carry higher risk in the LQT1 population (6). Nonsense mutations are expected to be non-functional and, when co-expressed with wild type subunits, not to affect wild-type KCNQ1 protein function. We also evaluated the expected effect of nonsense mutations (0.5 WT) (Table 2) and compared it to the effect of the 17 missense mutations. The functional effect observed was mild, consistent with the published milder clinical phenotype of nonsense mutations (6). The location of the mutations included in our study is shown in Fig. 1.

Electrophysiological parameters were obtained from expression of wild-type and mutant human KCNQ1 channel subunits together with the auxiliary KCNE1 subunit in *Xenopus laevis* oocytes at room temperature (see supplementary material for details). Wild-type and mutant KCNQ1 subunits were expressed at a 1:1 ratio to mimic the dominant nature of the disease, where both alleles are expressed in patients. The oocyte system allows control of the expression levels in each individual cell, producing low variability of current levels. Four mutant channels (G168R, S225L, R243C and V254M) were also expressed in the HEK293T mammalian cell line and yielded currents with the same activation and deactivation rates as in the oocyte system (Figure S2). Currents levels were decreased in the mammalian cells by approximately 30% for all mutants tested, but the proportion between mutant and WT currents was maintained. Our results indicate that the channel expression in *Xenopus laevis* oocytes can be used to study the rate of activation, deactivation impairment of IKs and relative changes in current and offers lower cell to cell variability, which is particularly important when a large number of mutants are being studied.

Changes in channel current (I_{mut} / I_{WT}), channel rate of activation (τ_{act} / $\tau_{act\text{-}WT}$) and channel rate of deactivation (τ_{deact} / $\tau_{deact\text{-}WT}$) were obtained for channels expressing mutant KCNQ1 subunits (Table 2). All 14 mutations found in the transmembrane region (S1-S6 domains) displayed a partial dominant negative response (I_{mut}/I_{WT} < 1). Consistent with a dominant negative response, these mutations also show significant changes in other channel gating parameters. Changes in maximal conductance (Gmax/Gmax-WT) and voltage dependence obtained from the Boltzmann fit of channel voltage dependence of activation curve (ΔV1/2 and k/k-WT) are shown in Table S1.

Correlation of QTc prolongation in mutation carriers to mutation-specific electrophysiology

Prolonged QTc_m in the population was associated with channels with smaller currents (I_{mut}) and slower activation (τ_{act}), but there was no correlation with changes in channel deactivation (τ_{deact}) (Figure 2). In a multivariate regression model, with QTc_m as a function of changes in current (I_{mut} / I_{WT}) and channel rate of activation (τ_{act} / $\tau_{act\text{-}WT}$), only decrease in current contributed independently to the QTc_m ($p=0.016$) whereas channel rate of activation did not ($p=0.25$). QTc_m showed limited or no correlation to the changes caused by the mutations in the voltage dependence of activation of the channel and maximal conductance (see Table S2 in the Supplementary Material).

Contribution of mutation-specific electrophysiology to the risk of cardiac events

We tested for the association of channel parameters with cardiac events, which included syncope (transient loss of consciousness that is abrupt in onset and offset),

aborted cardiac arrest (ACA) requiring defibrillation, and sudden cardiac death (unexpected sudden death without a known cause, SCD), whichever occurred first. Mutant channels with slower activation were significantly associated with an increased rate of cardiac events before age 30 (p=0.017), whereas the association with a decrease in channel current was only borderline significant (p=0.065) (Figure 2). Kaplan-Meier event free survival rate showed limited or no correlation with the mutation-induced changes in the voltage dependence of activation and maximal conductance (see Table S2s in the Supplementary Material).

In a multivariate Cox analysis, the median increase in rate of activation ($\tau_{act}/\tau_{act\text{-}WT}$ > 1.20) contributed to cardiac risk both univariately and independently of conventional risk markers such as individual patient QTc, gender and treatment with β-adrenergic receptor blockers (Table 3A, Figure 3A). The median decrease in I_{mut} and τ_{deact} was 50% and 20%, respectively. Neither changes in current (I_{mut}/I_{WT}, HR =1.07 [0.76 - 1.52], p=0.69) nor deactivation time (τ_{deacct} / $\tau_{deacct\ -WT}$, HR = 1.28 [0.90 - 0.63], p=0.55) contributed in the multivariate models.

Individual QTc is the main clinical parameter used in the assessment of cardiac risk for LQT patients. A baseline QTc of over 500 ms is an independent risk factor for cardiac events in LQTS (2, 13). In a secondary analysis shown in Table 3B, we excluded subjects with a severely prolonged QTc, defined as QTc >= 500 ms. A QTc >= 500 was found in 108 of 327 patients with a known QTc. In addition, 67 patients were obligate carriers of a mutation but died before having an ECG recorded; they were also excluded from this analysis. The remaining 212 patients were included. Mutant channels with slow channel activation (τ_{act} / $\tau_{act\text{-}WT}$ > 1.20) remained a strong predictor for cardiac events in patients with QTc < 500 ms, while a more pronounced QTc prolongation (QTc ≥ 470) did not predict increased risk of cardiac events (see Table 3B and Figure 3B).

The KCNQ1(V254M) mutant subunit strongly affected the channel activation time (τ_{act} / $\tau_{act\text{-}WT}$ =1.82). In order to classify the mutations into slow (τ_{act} / $\tau_{act\text{-}WT}$ > 1.20) and fast (τ_{act} / $\tau_{act\text{-}WT}$ <= 1.20) activating channels, the median value of the distribution of change in τ_{act} was calculated. After exclusion of channels containing KCNQ1(V254M), the median increase in τ_{act} was 20% for the remaining mutant channels. Exclusion of any individual mutation from the analysis did not significantly alter the results, indicating that no individual mutation drove the increase in cardiac risk observed for slow activating channels. To illustrate this, we show the stronger effect observed, due to the exclusion of the slowest activating channel, KCNQ1(V254M). With the separate analysis of KCNQ1(V254M), slow activating channels remained a strong predictor of cardiac events for the remaining study population and for patients with QTc<500 ms (Table 4, Figure 3C).

IKs activation is faster after stimulation by protein kinase A (PKA) and at higher temperatures (14). To determine whether the differences in activation time course recorded at room temperature in unstimulated cells (Table 1) are also observed at physiological temperatures and after PKA stimulation, we measured changes in activation time course caused by increasing temperature and after PKA activation for channels formed by wild type and wild type co-expressed with mutant subunits (G168R, S225L, R243C and V254M) in HEK293T cells. We measured activation time course when temperature was raised from 22^{o}C to 37^{o}C (Figure S3) and before and after application of the PKA activator forskolin (Figure S4). For all channels, activation time course at 37^{o}C and after PKA activation were faster, consistent with the previously reported data for the wild type channel. Both temperature and PKA mediated changes were not significantly different between wild type and mutant channels, indicating that

channels with slow kinetics of activation will remain slower than wild type channels under both conditions.

Modeling of early after depolarization in response to premature beats

To investigate the potential role of altered channel kinetics in generating pro-arrhythmic events, we use a mathematical reconstruction of a humanized model of the cardiac action potential based on the canine endocardium model of Flaim-Giles-McCulloch (FGM) (15) (for details see supplementary Material). We chose this model over others, including some based on human data, because the model formulation contains a more advanced representation of Ca^{+2} release mechanisms and reproduces large differences in epicardial, mid-myocardial and epicardial AP shapes, including rate-dependent changes in action potential duration.

First, we generated a train of endocardium action potentials paced at 1Hz and showed that slow channel activation in the range observed in the mutants studied (Table 2) can cause prolongation of action potential (Figure 4A). Second, to investigate the mechanism of arrhythmia generation in slow activating channels, we compared action potentials in cells with slow activating IKs channels and channels with decreased conductance, which caused an equivalent prolongation of the action potential. We imposed high β-adrenergic stimulation because arrhythmias are generally triggered during exercise for LQT1 patients (16). Although the exact mechanism of arrhythmias is not known, in experimental studies in canine drug-induced LQT1, the ventricular arrhythmia Torsade de Point (TdP) can be reproducibly triggered by β-adrenergic stimulation (17). Moreover, this study showed that TdP is preceded by systolic after-contractions, presumably from early after depolarizations that were found to occur predominately in the endocardium but not the epicardium.

In our simulation studies, endocardial cells with β-adrenergic drive showed EADs under the fast pacing protocol with one premature beat. Both decreases in channel conductance (Gmax = 0.65) and activation rate (τ_{act}=1.75) prolonged action potential duration (Fig.4A). For channels where conductance alone was decreased, premature beats caused an early after depolarization. For slowly activating channels the premature beat caused early after-depolarizations associated with a more prolonged depolarization and incomplete depolarization following the early after-depolarization (Fig.4B). Our results suggest that the slow repolarization of the cardiomyocytes caused by slow IKs activation affects the ability of the cell to recover from early after-depolarizations, potentially contributing to arrhythmogenesis. hese results are consistent with our clinical data showing that slow activation of IKs increases cardiac risk for patients independent of QTc prolongation.

Discussion

In this study, we investigated the association between conventional measures of ion channel function from expression studies and the clinical phenotype in LQT1 subjects with a verified KCNQ1 channel mutation. Prolonged QTc in carriers of the mutation was highly correlated with decreased channel current magnitude. Despite this, channel current amplitude correlated poorly with the risk of cardiac events in the carriers (syncope, aborted cardiac arrest or sudden death). In contrast, mutations causing a slow activation of the channel were strongly associated with increased risk for cardiac events. In patients with modest QTc prolongation (<500 ms), slow channel activation remained a strong independent predictor for cardiac events, while the QTc interval carried no predictive value. Thus, knowledge of the effect of the mutation on the channel rate of activation may help to identify individuals at an increased risk of cardiac events independent of clinical risk factors, and this may be especially important in the large

group of LQT1 patients presenting with modest QTc prolongation. The appropriate clinical care for LQT1 patients with modest QTc prolongation is not well established, with many patients remaining untreated. Identification of high risk mutations in this population can lead to more aggressive treatment in the population at risk and better patient care.

Mutations with a dominant negative effect on channel function have been shown to be associated with an increase in cardiac risk (6). Nonetheless, several previous studies have reported a poor correlation between current magnitude and the observed QTc interval in patients harboring the mutation(7-9). In particular, Wang and colleagues compared median QTc in patients to decrease in current for five LQT1 mutations, three of which were studied in the present study (9). Despite a decrease in current similar to that reported here, QTc_m prolongation for those patients did not significantly correlate to current decrease. This difference may have been a result of the low number of LQT1 mutations and/or subjects. We found a high inverse correlation between the measured mutant current magnitude and the median value for the observed QTc in carriers. However, for almost all mutations, carriers exhibited QTc durations over a broad range. This is a common finding(18) that indicates substantial influence of other modifiers on the QT interval and underscores the need for large populations in this type of study.

The mutation V254M prolonged τ_{act} excessively compared to 16 other mutations in this study. This is in agreement with previously results(19), and reports that the S4-S5 linker is important for K^+ channel gating (9, 19-21). However, as illustrated in Figure 1, mutations causing changes in τ_{act} > 20% and arrythmias were found at several other locations in the subunit such as the S4, S5 and S6 transmembrane domains as well as the pore region. For instance, A341V, previously associated with high cardiac risk (22, 23), also results in channels with slower activation rate. Removal of each individual

mutation from the analysis did not significantly alter the results, indicating that slow activation is a robust predictor of cardiac risk in the study population.

Although decrease in current and gmax, slower activation, faster deactivation, and shifts in voltage dependence of activation are expected to contribute to loss of channel function, here we showed that only slower τ of activation predicts cardiac risk in this patient population independently from patient QTc. To study the mechanism underlying the pro-arrhythmic state, we introduced slow activating IKs channels into a cardiomyocyte action potential model with simulated β-adrenergic stimulation. In a rapid pacing protocol with a premature beat, cells with channels having slow activation rate showed prolonged early after depolarizations and incomplete depolarization on the subsequent beat. Our simulation shows that both slow activation and decrease in conductance can similarly prolong action potential duration. Nonetheless, impaired recovery from early after depolarizations is observed for slow activating channels, suggesting that channel activation rate affects the ability to effectively repolarize the membrane. Both early after depolarizations and heterogeneity of action potential durations are thought to foster TdP (24). However, the precise mechanism of generation of whole heart arrhythmias is not yet clear.

We found that several mutations, with both severe and mild clinical phenotype, significantly altered the rate of deactivation. In previous studies, a faster rate of channel deactivation was found to be associated with channel dysfunctions, leading to a severe form of LQT1(25) and atrial fibrillation(26). During β-adrenergic stimulation, IKs channel deactivation is slowed (in addition to channel activation being accelerated). This regulation is thought to be important for the regulation of cardiac repolarization in response to increased heart rate (27). Our study found that changes in the basal rate of deactivation caused by LQT1 mutations did not correlate with either the median resting

QTc interval or with risk of cardiac arrhythmias, suggesting that impairment of current accumulation at high heart rates does not underlie the arrhythmias in LQT1.

Some mutations were only found in 10 subjects, which make assessment of the survival rate in these subjects less accurate. Also, some of the mutations were only found in members of one family, making other genetic traits possible confounders. However, the models in this study are adjusted by a jackknife approach, the covariance sandwich estimator, which removes members of each family from the model one by one, making the reported p values conservative. On top of this, we treated the mutation with the most radical results independently, so we believe the reported results are robust.

The *Xenopus laevis* oocyte system is a simple, cost effective and higher throughput technique than other heterologous expression systems. Here we show that it captures the changes in both current activation and deactivation rates and current decrease, reflecting changes observed in the mammalian system. We showed that the changes measured in the oocyte system can be used to predict ion channel cardiac risk. Our data suggest that measurement of ion channel function in this system can be extended to assess the cardiac risk of the hundreds of known mutations associated with LQT1, for which limited clinical data are available.

The occurrence of syncope and cardiac arrest is quite variable in LQT1, and proper risk stratification is needed in order to optimize patient treatment (6, 28-30). ß-adrenergic blockers are the treatment of choice for preventing cardiac events for patients with LQT1. Cardioverter defibrillator (ICD) therapy may be offered to patients who remain symptomatic despite β-adrenergic blocker therapy (28-30). However, this is an invasive procedure that may be associated with technical difficulties (especially in young children) and complications. Risk stratification approaches to identify LQTS patients who have a high-risk for cardiac arrhythmias are currently based mostly on the

phenotypic expression of the disease (assessed the magnitude of prolongation of QTc duration and clinical symptoms), and may therefore fail to identify high-risk patients with a moderate-range QTc , who comprise approximately 70% of the LQTS population (31). Our results will allow improved risk stratification for LQT1 patients. Specifically, β-blocker treatment may be indicated for patients with slow activating channels, despite the lack of clinical symptoms and the presence of a moderately prolonged QTc. Furthermore, our findings suggest that patients who carry mutations that are associated with slow activating channels should be carefully followed, regardless of additional risk factors, with more invasive interventions (including ICD implantation or left cardiac sympathetic denervation) if symptoms occur during medical therapy. In addition, our results may prove useful in assessing drug-induced cardiac risk for drugs that affect channel activation time course.

In conclusion, prolonged QTc values were correlated with decrease in ion channel current caused by the mutation. In addition, a slower rate of channel activation was significantly associated with an increased risk of cardiac events, independent of clinical measures such as gender, QTc and β-adrenergic blocker treatment. These associations were significant in the large group of patients with QTc < 500 ms, comprising the majority of LQT1 patients, for which the QTc interval provide little prognostic information. Thus, mutation-induced changes in the rate of IKs activation may provide an important tool for the risk assessment and management of LQTS patients and is the first step toward a mutation-specific risk stratification for Long QT patients. Our findings also suggest that development of drugs that affect kinetics of channel activation may be beneficial for LQT1 patients

MATERIALS AND METHODS

An expanded Methods section is available in the Online Data Supplement

Population

The population involved patients with either genetically confirmed LQT1 mutations or if they had died suddenly at a young age of suspected LQTS and were from a family with a genetically confirmed mutation. Patients were drawn from 4 LQTS registries: the U.S. part of the International LQTS Registry (n=319), the Netherlands LQTS Registry (n=44), the Japanese LQTS Registry (n=29), and the Danish LQTS Registry (n=1). To evaluate the clinical course of carriers with each mutation, we included mutations with at least 10 subjects. We identified patients with 17 different KCNQ1 missense mutations. For correlation with values for measures on the wild type KCNQ1/KCNE1 channel, we included 480 family members from the U.S. part of the International LQTS registry who

tested negative for LQT1 and not positive for any other LQTS genotype. All subjects or their guardians provided informed consent for the genetic and clinical studies.

The patients were enrolled during childhood, adolescence or, for a few individuals, during adulthood. The clinical course from birth up to enrollment was then reconstructed and the individual was followed prospectively from that point. This method allows modeling the clinical course from date of birth.

Genotype characterization

The KCNQ1 mutations were identified with the use genetic tests performed in academic molecular-genetic laboratories including the Functional Genomics Center, University of Rochester Medical Center, Rochester, NY; Baylor College of Medicine, Houston, TX; Mayo Clinic College of Medicine, Rochester, MN; Boston Children's Hospital, Boston, MA; Laboratory of Molecular Genetics, National Cardiovascular Center, Suita, Japan; Department of Clinical Genetics, Academic Medical Center, Amsterdam, Netherlands; and Statens Serum Institut, Copenhagen, Denmark. For the proband in each family, the 5 most common LQT loci (KCNQ1, KCNH2, SCN5A, KCNE1 and KCNE2) were fully sequenced to identify the mutation by comparing the sequence with sequence of healthy individuals without LQT. Once mutation was identified, other family members KCNQ1 gene was sequenced, to confirm the presence or absence of the mutation.

Phenotype characterization

The ECG parameters were obtained from the baseline ECG recorded at the time of enrollment in each of the registries. The QT and R-R intervals were measured in milliseconds, with QT corrected for heart rate by Bazett's formula (QTc). A small minority of individuals died suddenly before an ECG was recorded. Follow-up was

censored at age 41 years to avoid the influence of coronary. In all 4 registries, clinical data were collected on prospectively designed forms for demographic characteristics, personal and family medical history, ECG findings, therapy, and end-points during long-term follow-up. Data common to all 4 LQTS registries involving genetically identified patients with type-1 LQTS were electronically merged into a common database for the present study.

Endpoints

LQTS-related cardiac events included syncope, defined as transient loss of consciousness. abrupt in onset and offset, aborted cardiac arrest (ACA) requiring defibrillation, and sudden cardiac death (unexpected sudden death without a known cause, SCD), whichever occurred first. Information on end-point events was determined from the clinical history ascertained by routine follow-up contact with the patient, family members, attending physician, or the medical records. Syncope has been shown to be a major predictor and an excellent surrogate for cardiac death (32). The number of events are as follows: (176 total): syncope = 149, ACA = 9, SCD = 18. No implantable cardioverter defibrillator events were recorded in this population.

Electrophysiology

The electrophysiological parameters were obtained from expression of wild-type and mutant human KCNQ1 channel subunits at a ratio 1:1 in *Xenopus laevis* oocytes or HEK293Tcells. The auxiliary KCNE1subunit was also co-expressed in all experiments. The procedure is explained in detail in the supplementary data.

To assess the effect of the expression of the mutant channel subunit on the current magnitude we measured the current at +40 mV after 4s depolarization from -80 mV (I_{mut}). To measure the voltage dependence of channel activation, we measured the IKs tail current at -40 mV after depolarization to a series of voltage steps from -50 to +80 mV every 10 mV. A Boltzmann fit ($G = g_{max}/(1 + \exp[-(V - V_{1/2})/k)$ of this data was used to determine 1) the steepness or slope factor (*k*), 2) the voltage that elicits half of the maximal activation ($V_{1/2}$) of activation and 3) the maximal conductance (g_{max}). The $V_{1/2}$ and *k* values indicate channel sensitivity to activation by voltage. Time constant for activation (τ activation: τ_{act}) and for deactivation (τ deactivation: τ_{deact}) were determined by fitting the activation current and tail current with a single exponential. Human IKs channels activated to +40mV depolarizing voltage are well fit by a single exponential ($R>0.98$ for all data points), although double exponentials improve the fit ($R>0.99$). Notheless, for the purposes of this study, a single exponential fit was sufficient to capture the increase in cardiac risk, so we used the simplest model. This is illustrated in detail in Figure 1s in the supplementary data.

Statistics

The values of $I_{mut,}$ τ_{act}, τ_{deact}, $V_{1/2}$, and g_{max} measured for channels expressing the mutant subunits (0.5 KCNQ1: 0.5 KCNQ1 mut: 1.0 KCNE1) were compared to the control mimicking the haploinsufficient phenotype (0.5 KCNQ1: 1.0 KCNE1) and changes in these parameters are reported as mean ± SE. The distributions of QTc intervals measured in carriers of different mutations were not normally distributed and are expressed as median (range). Unpaired Student's t-test was performed to compare two data sets. For multiple comparisons, one-way ANOVA followed by posthoc Tukey test or Dunnett's test was performed. Statistical significance was set as a *P* value of <0.05.

Several approaches were used to compare the characteristics of the channels formed with the mutant subunits with the clinical observations in the study population. To obtain measures of correlation that were independent of the varying population size of the carriers with each mutation, we compared the average biophysical parameters with median values of QTc and the 30 year Kaplan Meier survival rates to first cardiac event for the carriers of each mutation using linear regression. The 30 year Kaplan Meier limit was chosen due to the low event rate after this time point. Next, linear regression was used to test how well each channel characteristic influenced the variability of the absolute QTc measured at baseline in all carriers. Confidence intervals and *p*-values were adjusted for the sample size. Only parameters that were significant in the linear regression models were included in the further analysis. Cox proportional hazards survivorship model was used to evaluate the independent contribution of the biophysical parameters compared to clinical and genetic factors to the first occurrence of time-dependent cardiac events from birth through end of follow-up at age 40 years. Since the mutation V254M were found to have radically altered parameters compared to the 16 other mutations, we treated carriers of V254M as an independent risk group. Since the slope of voltage dependence of activation curve (*k*) was largely unchanged by the mutations studied, this parameter was not included in the analyses. The remaining ion channel parameters were dichotomized at the median (50%) values according to the frequency distributions in the carriers excluding V254M carriers. To account for the influence of family membership between individuals, all Cox models were fit using a jackknife approach, the covariance sandwich estimator (33) which removes members of each family from the model one by one. The genotype-negative family members were not included in the Cox-models. Patients who

died suddenly at a young age from suspected LQTS and who did not have an ECG for QTc measurement were identified in the Cox models as “QTc missing”.

Modeling

The cell model is adapted from the Flaim-Giles-McCulloch (FGM) reconstruction of the canine cardiac cell (34). The IKs current is described by a Hodgkin-Huxley type formulation (see supplementary data for detail of current formulation). This is a typical type of formalism in cardiac models and provides as compact and computationally efficient representation of the complex behavior of channel gating kinetics (for review, see (35)). We modified the wild type IKs current parameters in the model to better correspond to the electrophysiological data collected in this study. Specifically the formulation is changed so that current is proportional to xKs, the infinity gating variable, to the first power. Other changes were made to the time constants to make the channel properties more similar to experimental characterizations (see Supplementary Materials details). These modifications allow the relative changes in IKs as assessed in the electrophysiology section to be mapped into model studies in a straight forward fashion (e.g., a 50% increase in τ_{act} for a given mutant in the experimental study was simulated by a 50% increase in τ_{act} in the model). β-Adrenergic stimulation simulates increases in IKs current densities and the increased Ca^{2+} load observed experimentally during β-adrenergic stimulation (for details see supplementary materials)

The pacing protocol consists of 40 beats at a 1000 ms interval and 30 beats at 500 ms interval to bring the model to steady state, followed by one premature beat at after 350

ms and then return to the initial rate. The premature beat produces a decreased Ca^{2+} transient that is followed by a larger Ca transient on the subsequent beat.

Table 1. Patient characteristics by mutations

n = number of patients, GTNF = Genotype negative family members.

Mutation	n	Families	Registries 1=US, 2=Nederland 3=Japan 4=Denmark	Gender (% males)	QTc (ms) median (range)	Beta blockers started	References
G168R	68	7	1	41 %	475 (410-660)	35 %	(36), (37)
Y184S	14	3	2	43 %	470 (450-520)	64 %	(38)
S225L	14	4	1, 2	29 %	475 (450-500)	36 %	(39)
R243C	13	5	1,3	15 %	495 (420-680)	38 %	(19), (40)
V254M	62	4	1,4	48 %	500 (450-590)	53 %	(9)
L266P	24	5	1	25 %	490 (390-580)	33 %	-
G269S	41	5	1, 3	49 %	480 (410-650)	46 %	(41)
W305S	16	1	1	38 %	430 (390-480)	69 %	(42)
T312I	17	2	1	47 %	500 (410-600)	60 %	-
G314S	19	5	1, 2, 3	53 %	485 (420-630)	32 %	(43)
Y315C	10	1	1	40 %	450 (440-470)	20 %	(39, 41)
A341E	10	1	1	40 %	460 (410-700)	50 %	(9, 41)
A341V	21	6	1, 2, 3	38 %	490 (410-560)	57 %	(9, 18, 22, 23, 44, 45)
S349W	15	3	1	53 %	450 (390-510)	53 %	-
R591H	19	3	1, 3	53 %	470 (420-600)	47 %	(46, 47)
R594Q	14	4	1, 2	43 %	455 (400-760)	43 %	(46)
D611Y	10	1	3	50 %	410 (370-460)	0 %	(48)
GTNF (WT)	48	90	1	47 %	420 (340-550)	8 %	-

Table 2. Changes in ion channel parameters caused by LQT1 mutation. Mutant channel subunits are expressed together with wild type subunits and the auxiliary KCNE1 subunits at a ratio 0.5 Q1WT: 0.5 Q1mut: 1.0 E1. Values are normalized by the values measured in the channels that mimic the haploinsufficient phenotype (0.5 WT). The wild-type channel is also measured as a comparison (WT). * marks values that are significantly different from the channel mimicking the haploinsufficient phenotype (0.5 WT) ($p \leq 0.05$). n = number of cells measured. I = activated current measured at +40 mV after 4s depolarization, τ_{act} = single exponential fit of the activation current, τ_{deac}= single exponential fit of the current deactivation.

	I / I_{WT}			$\tau_{act} / \tau_{act\text{-}WT}$			$\tau_{deact} / \tau_{deact\text{-}WT}$		
Mutation	**n**	**mean**	**SE**	**n**	**mean**	**SE**	**n**	**mean**	**SE**
WT	36	1.39*	±0.08	38	0.93*	±0.03	52	1.02	±0.03
0.5 WT	94	1.00	±0.03	94	1.00	±0.02	96	1.00	±0.02
G168R	24	0.39*	±0.02	25	1.21*	±0.04	24	0.90	±0.04
Y184S	18	0.71*	±0.08	18	1.14*	±0.03	18	1.02	±0.03
S225L	22	0.61*	±0.05	24	1.33*	±0.05	23	0.74*	±0.03
R243C	30	0.42*	±0.03	34	1.18*	±0.03	35	0.79*	±0.02
V254M	24	0.39*	±0.02	27	1.82*	±0.08	26	1.13*	±0.04
L266P	24	0.29*	±0.02	25	1.25*	±0.04	25	0.83*	±0.03
G269S	24	0.52*	±0.03	26	1.16*	±0.03	27	0.68*	±0.03
W305S	37	0.38*	±0.02	37	1.19*	±0.06	39	0.71*	±0.03
T312I	20	0.20*	±0.02	21	1.30*	±0.05	21	0.76*	±0.03
G314S	32	0.32*	±0.02	17	1.25*	±0.06	20	0.90*	±0.03
Y315C	24	0.62*	±0.04	24	1.03	±0.04	24	0.78*	±0.03
A341E	27	0.41*	±0.04	28	1.15*	±0.06	30	0.93	±0.03
A341V	24	0.56*	±0.07	26	1.21*	±0.04	26	0.78*	±0.03
S349W	25	0.73*	±0.06	27	1.31*	±0.05	29	1.00	±0.04
R591H	25	0.95	±0.10	25	0.97	±0.03	32	0.99	±0.02
R594Q	26	0.99	±0.03	25	0.94	±0.04	30	0.97	±0.03
D611Y	27	1.47*	±0.03	25	0.87	±0.06	28	0.95	±0.07

Table 3 Multivariate Cox models. Channel activation time (τ_{act} / $\tau_{act\text{-}WT}$ > 1.20) is dichotomized at median values. **A**: shows results from the entire population. **B:** shows results on the 212 patients with QTc < 500 ms. * The models are adjusted for male gender ages 0-12 years and time-dependent beta-blocker therapy which significantly contributed to all multivariate results.

A. Cox model including all 387 patients*

Parameter	*Hazard ratio*	*95% CI*	*p-value*
τ_{act} / $\tau_{act\text{-}WT}$ > 1.20	2.02	1.44 - 2.82	<0.001
QTc ≥ 500 ms	1.86	1.32 - 2.62	<0.001

B. Cox model including only the 212 patients with QTc < 500 ms*

Parameter	*Hazard ratio*	*95% CI*	*p-value*
τ_{act} / $\tau_{act\text{-}WT}$ > 1.20	2.22	1.35 - 3.63	0.002
QTc ≥ 470 ms	0.89	0.56 - 1.41	0.62

Table 4 Multivariate Cox models with carriers of V254M modeled individually. Channel activation time (τ_{act} / $\tau_{act\text{-}WT}$ > 1.20) is dichotomized at median values. **A**: shows results from the entire population. **B:** shows results on the 212 patients with QTc < 500 ms. * The models are adjusted for male gender ages 0-12 years and time-dependent beta-blocker therapy which significantly contributed to all multivariate results.

A. Cox model including all 387 patients*

Parameter	*Hazard ratio*	*95% CI*	*p-value*
τ_{act} / $\tau_{act\text{-}WT}$ > 1.20	1.55	1.08 - 2.23	0.016
QTc ≥ 500 ms	1.64	1.16 - 2.31	0.004
V254M mutation carrier	2.91	1.75 - 4.86	<0.001

B. Cox model including only the 212 patients with QTc < 500 ms*

Parameter	*Hazard ratio*	*95% CI*	*p-value*
τ_{act} / $\tau_{act\text{-}WT}$ > 1.20	1.80	1.06 – 3.03	0.029
QTc ≥ 470 ms	0.82	0.51 - 1.32	0.42
V254M mutation carrier	3.03	1.84 - 4.98	<0.001

FIGURE LEGENDS:

Figure 1. Location of the mutations included in the study. Black circles, Mutations in the study; yellow: $I_{mut} / I_{Kact\text{-}WT} < 1.00$ (partially dominant-negative); green: $\tau_{act} / \tau_{act\text{-}WT} > 1.20$ (increased more than 20%); blue: $\tau_{deact} / \tau_{deact\text{-}WT} < 0.80$ (decreased more than 20%)

Figure 2. **Results from simple linear regression.** Simple linear regression between ion channel characteristics and either the observed median QTc (left) or the observed 30-year Kaplan Meier survival rates (right) for carriers of each mutation. (**A)** Correlation between changes in ion channel current (I_{mut}/I_{WT}) and median QTc (left) or 30-year Kaplan Meier survival rates (right). (**B)** Correlation between rate of current activation (τ_{act}/τ_{actWT}) and median QTc (left) or 30-year Kaplan Meier survival rates (right). (**C)** Correlation between changes in rate of current deactivation ($\tau_{deact}/\tau_{deactWT}$) and median QTc (left) or 30-year Kaplan Meier survival rates (right)

Figure 3. Contribution of slow activation and QTc for the cumulative risk of first cardiac event. Kaplan Meier graphs showing the probability of first cardiac event before age 30 in carriers of mutations. **A:** *Left*: Patients with QTc<500ms and QTc>=500ms have significantly different cardiac risk. *Right*: Patients carrying mutations that produce fast ($\tau_{act} / \tau_{act\text{-}WT} \leq 1.20$) and slow ($\tau_{act} / \tau_{act\text{-}WT} > 1.20$) activating channels have significantly different cardiac risk. (n=387) **B.** For patients with moderate prolongation of QTc. *Left*: Patients with QTc<470ms and 470=<QTc<500ms do not show differences in cardiac risk. QTc=470 is the median QTc value for this population. *Right:* Patients carrying mutations that produce fast ($\tau_{act} / \tau_{act\text{-}WT} \leq 1.20$) and

slow (τ_{act} / $\tau_{act\text{-}WT}$ > 1.20) activating channels have significantly different cardiac risk (n=212). **C.** Kaplan Meier graphs showing the probability of first cardiac event before age 30 in carriers of mutations with τ_{act} / $\tau_{act\text{-}WT}$ ≤ 1.20, τ_{act} / $\tau_{act\text{-}WT}$ > 1.20 with adjustment for carriers of V254 (τ_{act} / $\tau_{act\text{-}WT}$ = 1.82). *Left*: all patients. *Right*: patients with QTc < 500 ms.

Figure 4. Effect of slow channel activation on modeled cardiac action potential. A: Cardiac action potential model with wild-type IKs channels, IKs channels with slower activation as indicated. What is the top, middle and lower graph? Specify. **(B)** Effect of a premature beat on modeled action potential. Cardiac action potential model with wild-type IKs channels, IKs channels with decreased conductance (0.65 gmax) and/or IKs channels with slow activation (1.75 τ_{act}) as indicated. Note that before the premature beat, the action potentials for 0.65 gmax and 1.75 τ_{act} virtually overlay. Cells with channels with slow activation show an increase prolongation of the action potential during early after depolarizations and incomplete depolarization following the premature beat. Stimulation rate of 2 Hz was used to mimic the fast heart rates seen during β-adrenergic stimulation.

Reference List

1. Wang Q, Curran ME, Splawski I, Burn TC, Millholland JM, VanRaay TJ, Shen J, Timothy KW, Vincent GM, de Jager T *et al.* (1996) *Nat Genet.* **12**, 17-23.
2. Priori, S. G., Schwartz, P. J., Napolitano, C., Bloise, R., Ronchetti, E., Grillo, M., Vicentini, A., Spazzolini, C., Nastoli, J., Bottelli, G. *et al.* (2003) *N. Engl. J. Med.* **348**, 1866-1874.
3. Sauer, A. J., Moss, A. J., McNitt, S., Peterson, D. R., Zareba, W., Robinson, J. L., Qi, M., Goldenberg, I., Hobbs, J. B., Ackerman, M. J. *et al.* (2007) *J. Am. Coll. Cardiol.* **49**, 329-337.

4. Hobbs, J. B., Peterson, D. R., Moss, A. J., McNitt, S., Zareba, W., Goldenberg, I., Qi, M., Robinson, J. L., Sauer, A. J., Ackerman, M. J. *et al.* (2006) *JAMA* **296**, 1249-1254.

5. Goldenberg, I., Moss, A. J., Peterson, D. R., McNitt, S., Zareba, W., Andrews, M. L., Robinson, J. L., Locati, E. H., Ackerman, M. J., Benhorin, J. *et al.* (2008) *Circulation* **117**, 2184-2191.

6. Moss, A. J., Shimizu, W., Wilde, A. A., Towbin, J. A., Zareba, W., Robinson, J. L., Qi, M., Vincent, G. M., Ackerman, M. J., Kaufman, E. S. *et al.* (2007) *Circulation* **115**, 2481-2489.

7. Bianchi, L., Priori, S. G., Napolitano, C., Surewicz, K. A., Dennis, A. T., Memmi, M., Schwartz, P. J., & Brown, A. M. (2000) *Am. J. Physiol Heart Circ. Physiol* **279**, H3003-H3011.

8. Murray, A., Potet, F., Bellocq, C., Baro, I., Reardon, W., Hughes, H. E., & Jeffery, S. (2002) *J. Med. Genet.* **39**, 681-685.

9. Wang, Z., Tristani-Firouzi, M., Xu, Q., Lin, M., Keating, M. T., & Sanguinetti, M. C. (1999) *J. Cardiovasc. Electrophysiol.* **10**, 817-826.

10. Jons, C., Moss, A. J., Lopes, C. M., McNitt, S., Zareba, W., Goldenberg, I., Qi, M., Wilde, A. A., Shimizu, W., Kanters, J. K. *et al.* (2009) *J. Cardiovasc. Electrophysiol.* **20**, 859-865.

11. Capra, J. A. & Singh, M. (2007) *Bioinformatics.* **23**, 1875-1882.

12. Valdar, W. S. & Thornton, J. M. (2001) *J. Mol. Biol.* **313**, 399-416.

13. Zareba, W., Moss, A. J., Schwartz, P. J., Vincent, G. M., Robinson, J. L., Priori, S. G., Benhorin, J., Locati, E. H., Towbin, J. A., Keating, M. T. *et al.* (1998) *N. Engl. J. Med.* **339**, 960-965.

14. Imredy, J. P., Penniman, J. R., Dech, S. J., Irving, W. D., & Salata, J. J. (2008) *Am. J. Physiol Heart Circ. Physiol* **295**, H1867-H1881.

15. Flaim, S. N., Giles, W. R., & McCulloch, A. D. (2007) *Heart Rhythm.* **4**, 768-778.

16. Schwartz PJ, Priori SG, Spazzolini C, Moss AJ, Vincent GM, Napolitano C, Denjoy I, Guicheney P, Breithardt G, Keating MT *et al.* (2001) *Circulation* **103**, 89-95.

17. Gallacher, D. J., Van de Water, A., van der Linde, H., Hermans, A. N., Lu, H. R., Towart, R., & Volders, P. G. A. (2007) *Cardiovascular Research* **76**, 247-256.

18. Brink, P. A., Crotti, L., Corfield, V., Goosen, A., Durrheim, G., Hedley, P., Heradien, M., Geldenhuys, G., Vanoli, E., Bacchini, S. *et al.* (2005) *Circulation* **112**, 2602-2610.

19. Franqueza, L., Lin, M., Shen, J., Splawski, I., Keating, M. T., & Sanguinetti, M. C. (1999) *J. Biol. Chem.* **274**, 21063-21070.

20. Sanguinetti, M. C. & Xu, Q. P. (1999) *J. Physiol* **514 (Pt 3)**, 667-675.

21. Tristani-Firouzi, M., Chen, J., & Sanguinetti, M. C. (2002) *J. Biol. Chem.* **277**, 18994-19000.

22. Heradien, M. J., Goosen, A., Crotti, L., Durrheim, G., Corfield, V., Brink, P. A., & Schwartz, P. J. (2006) *J. Am. Coll. Cardiol.* **48**, 1410-1415.

23. Crotti, L., Spazzolini, C., Schwartz, P. J., Shimizu, W., Denjoy, I., Schulze-Bahr, E., Zaklyazminskaya, E. V., Swan, H., Ackerman, M. J., Moss, A. J. *et al.* (2007) *Circulation*.

24. Aizawa, Y., Ueda, K., Scornik, F., Cordeiro, J. M., Wu, Y., Desai, M., Guerchicoff, A., Nagata, Y., Iesaka, Y., Kimura, A. *et al.* (2007) *J. Cardiovasc. Electrophysiol.* **18**, 972-977.

25. Arbour, L., Rezazadeh, S., Eldstrom, J., Weget-Simms, G., Rupps, R., Dyer, Z., Tibbits, G., Accili, E., Casey, B., Kmetic, A. *et al.* (2008) *Genet. Med.* **10**, 545-550.

26. Restier, L., Cheng, L., & Sanguinetti, M. C. (2008) *J. Physiol* **586**, 4179-4191.

27. Terrenoire, C., Clancy, C. E., Cormier, J. W., Sampson, K. J., & Kass, R. S. (2005) *Circ. Res.* **96**, e25-e34.

28. Priori, S. G., Napolitano, C., Schwartz, P. J., Grillo, M., Bloise, R., Ronchetti, E., Moncalvo, C., Tulipani, C., Veia, A., Bottelli, G. *et al.* (2004) *JAMA* **292**, 1341-1344.

29. Moss, A. J. (2003) *JAMA* **289**, 2041-2044.

30. Zareba, W., Moss, A. J., Sheu, G., Kaufman, E. S., Priori, S., Vincent, G. M., Towbin, J. A., Benhorin, J., Schwartz, P. J., Napolitano, C. *et al.* (2003) *Journal of Cardiovascular Electrophysiology* **14**, 1149-1153.

31. Zareba, W., Moss, A. J., Schwartz, P. J., Vincent, G. M., Robinson, J. L., Priori, S. G., Benhorin, J., Locati, E. H., Towbin, J. A., Keating, M. T. *et al.* (1998) *N. Engl. J. Med.* **339**, 960-965.

32. Lane, R. E., Cowie, M. R., & Chow, A. W. (2005) *Heart* **91**, 674-680.

33. Lin, D. Y. & Wei, L. J. (1989) *Journal of the American Statistical Association* **84**, 1074-1078.

34. Flaim, S. N., Giles, W. R., & McCulloch, A. D. (2007) *Heart Rhythm.* **4**, 768-778.

35. Reumann, M., Fitch, B. G., Rayshubskiy, A., Pitman, M. C., & Rice, J. J. (2009).

36. Ridefelt, P., Yokote, K., Claesson-Welsh, L., & Siegbahn, A. (1995) *Growth Factors* **12**, 191-201.

37. Jongbloed, R., Marcelis, C., Velter, C., Doevendans, P., Geraedts, J., & Smeets, H. (2002) *Hum. Mutat.* **20**, 382-391.

38. Jongbloed, R. J., Wilde, A. A., Geelen, J. L., Doevendans, P., Schaap, C., Van, L., I, van Tintelen, J. P., Cobben, J. M., Beaufort-Krol, G. C., Geraedts, J. P. *et al.* (1999) *Hum. Mutat.* **13**, 301-310.

39. Bianchi, L., Priori, S. G., Napolitano, C., Surewicz, K. A., Dennis, A. T., Memmi, M., Schwartz, P. J., & Brown, A. M. (2000) *American Journal of Physiology-Heart and Circulatory Physiology* **279**, H3003-H3011.

40. Baker, O. S., Larsson, H. P., Mannuzzu, L. M., & Isacoff, E. Y. (1998) *Neuron* **20**, 1283-1294.

41. Chen, Y. H., Xu, S. J., Bendahhou, S., Wang, X. L., Wang, Y., Xu, W. Y., Jin, H. W., Sun, H., Su, X. Y., Zhuang, Q. N. *et al.* (2003) *Science* **299**, 251-254.

42. Neyroud, N., Denjoy, I., Donger, C., Gary, F., Villain, E., Leenhardt, A., Benali, K., Schwartz, K., Coumel, P., & Guicheney, P. (1998) *Eur. J. Hum. Genet.* **6**, 129-133.

43. Du, R., Yang, J. G., Li, W., Gui, L., Yuan, G. H., Kang, C. L., Ren, F. X., & Zhang, S. Y. (2005) *Zhonghua Yi. Xue. Yi. Chuan Xue. Za Zhi.* **22**, 68-70.

44. Kobori, A., Sarai, N., Shimizu, W., Nakamura, Y., Murakami, Y., Makiyama, T., Ohno, S., Takenaka, K., Ninomiya, T., Fujiwara, Y. *et al.* (2004) *J. Cardiovasc. Electrophysiol.* **15**, 190-199.

45. Anastasakis, A., Kotta, C. M., Kyriakogonas, S., Wollnik, B., Theopistou, A., & Stefanadis, C. (2006) *Europace.* **8**, 241-244.

46. Tester, D. J., Cronk, L. B., Carr, J. L., Schulz, V., Salisbury, B. A., Judson, R. S., & Ackerman, M. J. (2006) *Heart Rhythm.* **3**, 815-821.

47. Grunnet, M., Behr, E. R., Calloe, K., Hofman-Bang, J., Till, J., Christiansen, M., McKenna, W. J., Olesen, S. P., & Schmitt, N. (2005) *Heart Rhythm.* **2**, 1238-1249.

48. Yamaguchi, M., Shimizu, M., Ino, H., Terai, H., Hayashi, K., Kaneda, T., Mabuchi, H., Sumita, R., Oshima, T., Hoshi, N. *et al.* (2005) *Clin. Sci. (Lond)* **108**, 143-150.

49. Acknowledgments: We thank Jaime Sorenson for her technical support. Funding:

Supported by NIH - R01(HL033843) , Mirowski-Moss Career Development Award at the University of Rochester Medical Center, Rochester (to C.J.), AHA

Postdoctoral Fellowship (09POST2310079) (J. O-U.) and Foreign Study Grant Award of Kanae Foundation (J. O-U.). Author contributions: CJ, JO-U performed experiments, data analysis and wrote the paper; CMBL guided design of experiments and analysis; WZ, AAMW, WS, JKK, NH provided clinical data and contribute to analysis interpretation. AJM, IG, SM and JLR performed clinical data analysis and contribute to analysis interpretation. MR and JJR performed computer simulation. Competing interests: The authors declare that they have no competing interests.

Supplementary data

Supplementary Material and Methods

Plasmids and Reagents

Human KCNQ1 and KCNE1 in pcDNA3.1(+) plasmid, were a gift from R.S. Kass and used as described (1). All Regents were purchased from Sigma-Aldrich Corporation unless otherwise indicated.

Molecular Biology

Human KCNQ1, KCNE1 were subcloned in the pGEMsh vector (modified from PGEMHE vector) for oocyte expression(1, 2). PCR based site direct mutagenesis was performed using PFU ultra DNA polymerase (Stratagene, La Jolla, CA). Construct sequences were confirmed by DNA sequencing (Cornell University, Ithaca, NY). cRNAs were transcribed using the “message machine” kit (Ambion, Austin, TX). RNA concentration was estimated using RNA markers (Invitrogen, Calrlsbad, CA).

Electrophysiology

Xenopus oocytes were harvested, dissociated and defolliculated by collagenase type I treatment. Mutant channel subunits were expressed in combination with wild type subunits to mimic heterozygous mutations. KCNQ1:KCNE1 cRNA was injected either at a molar ratio of 1:1 (2ng:0.4ng) or 0.5:1 (1ng:0.4ng) in order to mimic the haploinsuficient phenotype. Mutant KCNQ1 cRNA was injected at a molar ratio 1:1 (wild-type:mutant) or 1ng wild-type KCNQ1 : 1ng mutant KCNQ1 : 0.4ng KCNE1. Mutations with currents significantly different than the haploinsuficient control were considered dominant negative mutations. Whole-oocyte currents

were measured with a GeneClamp 500 amplifier (Axon Instruments, Union City, CA). Agarose-cushioned microelectrodes were used with resistances between 0.1 to 1.0 MΩ. Oocytes were constantly superfused with (in mmol/L): 91 NaCl, 2 KCl, 1 $MgCl_2$, 1.8 $CaCl_2$, 5 NaOH/HEPES (pH 7.5). Currents of the mutant channels (I_{Mut}) were evaluated 1 min after oocytes impailment. At least 10 oocytes of the same batch and 2-3 oocyte batches were used. One-way ANOVA followed by Dunnett's Post Hoc test was applied for the assessment of statistical significance when comparing the channel expressing the mutant subunits to wild type channel function. KCNE1 expressed by itself at the concentrations used for these experiments yielded currents at least 10 times smaller than any of the mutant currents measured. This current did not significantly affect our analysis of the expressed channels. Because I_{Ks} does not reach a steady level even after long depolarizations at room temperature, we constructed isochronal (t=8s) activation curves to determine the voltage dependence of I_{Ks}. Experiments using longer depolarizing pulses (18s compared to 2.7s) showed that length of the depolarizing pulse affects the voltage dependence of I_{Ks}, but relative shifts in the voltage dependence persists independent of the length of the pulse(3). All experiments were performed at room temperature.

HEK293T cells (generously provided by Dr. Keigi Fujiwara, University of Rochester) were maintained in high glucose (4.5 g/L) Dulbecco's modified Eagle's medium (Mediatech, Herndon, VA) supplemented with 10% fetal bovine serum (Equitech-Bio, Kerrville, TX) and 1% L-glutamax (Invitrogen) in a humidified incubator with 5% CO_2. Each mutant KCNQ1 was expressed in combination with WT-KCNQ1 to mimic heterozygous mutation. Mutant KCNQ1 plasmid was transfected with WT KCNQ1 and KCNE1 plasmids at the ratio of 0.5 ng mutant KCNQ1:0.5 ng WT-KCNQ1:1ng KCNE1. Each mutant current was compared to the current

observed from haplosuficient control channel (0.5 μg WT-KCNQ1: 1μg KCNE1 co-transfected with 0.5 μg pcDNA3.1(+) vector) or WT control channel (1 μg WT-KCNQ1: 1μg KCNE1) from the same passage cells. Cells were also co-transfected with 0.2 μg pEGFP-N1 (Clontech, La Jolla, CA) for positive identification of transfected cells by fluorescence. All transfections were done by using Fugene HD trasnfection kit (Roche, Mannheim, Germany). Cells were re-plated on small glass cover slide (VWR, West Chester, PA) coated with 0.02 % gelatin 24 hours after transfection by using Accutase (Innovative Cell technologies. Inc., San Diego, CA) and use for experiment 48 hours after transfection.

The composition of the extracellular solution for the I_{Ks} measurements was (in mmol/L): 145 NaCl, 5.4 KCl, 1. $MgCl_2$, 1.8 $CaCl_2$, 10 HEPES, 10 glucose (pH 7.40 adjusted by NaOH). The composition of the pipette solution was (in mmol/L): 130 K-aspartate, 11 EGTA, 1. $MgCl_2$, 1 $CaCl_2$, 10 HEPES, 5 K-ATP (pH 7.20 adjusted by KOH). Cell-plated small glass cover slides were placed on recording chamber (Warner Instruments, Hamden, CT) and perfused with the extracellular solution. All experiments were performed at room temperature (≅ 22°C) unless otherwise indicated. Application of the Forskolin (adenylyl cyclase activator)-contained extracellular solution was done by local ejection from a small-tipped pipette with ValveBank8 Perfusion System (AutoMate Scientific, Berkeley, CA). For investigating temperature-dependent changes in channel functions, extracellular solution were heated up to 37°C and applied by local ejection using In-line Solution Heater (Model SH-27R, Warner Instruments) controlled by Automatic Temperature Controller (Model TC-344B, Warner Instruments).

Action Potential model

The cell model is adapted from the Flaim-Giles-McCulloch (FGM) reconstruction of the canine cardiac cell (4). The IKs current is described by a Hodgkin-Huxley type formulation with an infinity function (XKs_inf) and a time constant function (XKs_tau). This is a typical type of

formalism in cardiac models and provides as compact and computationally efficient representation of the complex behavior of channel gating kinetics (for review, see (5)). Two critical changes were made in our model: 1) IKs current proportional to XKs_inf to the first power instead of second power in the original formulation. The change is made to match the electrophysiological data that were collected in this study and fit with XKs_inf to the first power. Hence there is an essentially a one-to-one correspondence between the experimental channel data and the modifications to the model parameters. 2) Ito1 and Ito2 are reduced to 50% and 0%, respectively, of their original values to match published human data (6, 7). These changes produce an AP shape that more resembles human than dog. 3) Parameters for voltage dependence of IKs conductance, activation time course and deactivation time course were changed to matched human IKs channel data (8, 9). IKs in human ventricles varies significantly in different studies and has been suggested to be strongly dependent on cell isolation techniques (9). We used IKs densities measured in the canine myocardium, which are consistent with the published reports in humans (9).

Formulation of IKs for computer model:

$$IKs = GKs \times xKs \times (V - EKs)$$

$$xKs\_inf = 1/(1 + \exp(-(V - 9.4)/11.8)$$

$$a1 = 0.0000719 \times V/(1 + \exp(-0.74V))$$

$$a2 = 0.000786 \times (V + 40)/(\exp(0.103(V + 40) - 1)$$

$$xKs\_tau = 1/(a1 + a2)$$

Because arrhythmias are generally triggered during exercise for LQT1 patients (10), we modeled a high state of β-adrenergic stimulation so that IKs current densities were effectively 2

times larger than the unstimulated case suggested by experimental studies (8, 11). To simulate the rise in the AP plateau and the increased Ca^{2+} load, we made two changes to the Ca-handling mechanisms (12). First the uptake of the sarco/endoplasmic reticulum Ca^{2+} -ATPase (SERCA) pumps are increased by increasing the forward rate (vmaxf) by 60% (13). Second, the influx via L-type channels is increased by decreasing the closure rate (gL) by 60% (14). The rationale is to simulate the effects of β-adrenergic stimulation that produces a gate mode with open times that are roughly twice that of the unstimulated case (12, 15, 16).

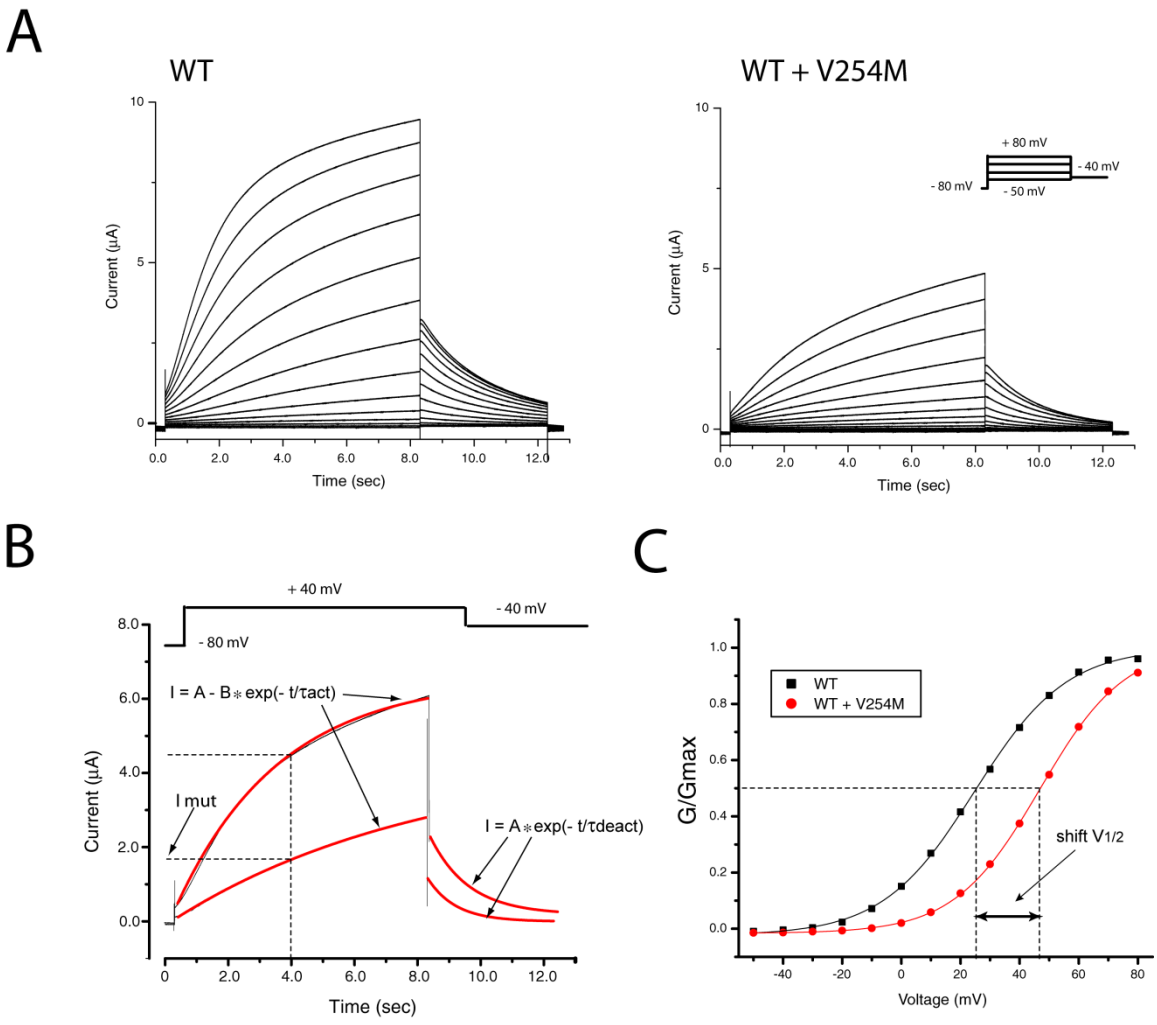

Fig. S1. Determination of ion channel characteristics. A: Typical ion channel current measured for *left*: wild-type (WT) and *right*: WT and mutant subunits co-expresssed at a 1:1 ratio. Currents were activated by 8s depolarizing steps from -50mV to +80 mV every 10mV from a -80mV holding potential. These were followed by a step to -40mV. **B:** Typical current trace of cells expressing the WT+V254M subunits showing a single-exponential fit to both activating and deactivating currents (τ_{act} and τ_{deact} were derived as shown). **C:** Typical plot of current measured at -40 mV immediately after depolarizing steps to the voltages indicated for channels formed with either WT or WT+V254M. Solid line is a Boltzmann fit of the plot. $V_{1/2}$ is the voltage that activates 50% of the maximum current and was obtained from the Boltzmann fit of the data. Plot was normalized to the maximal current. KCNE1 was co-expressed with the KCNQ1 subunits at a ratio 1:1.

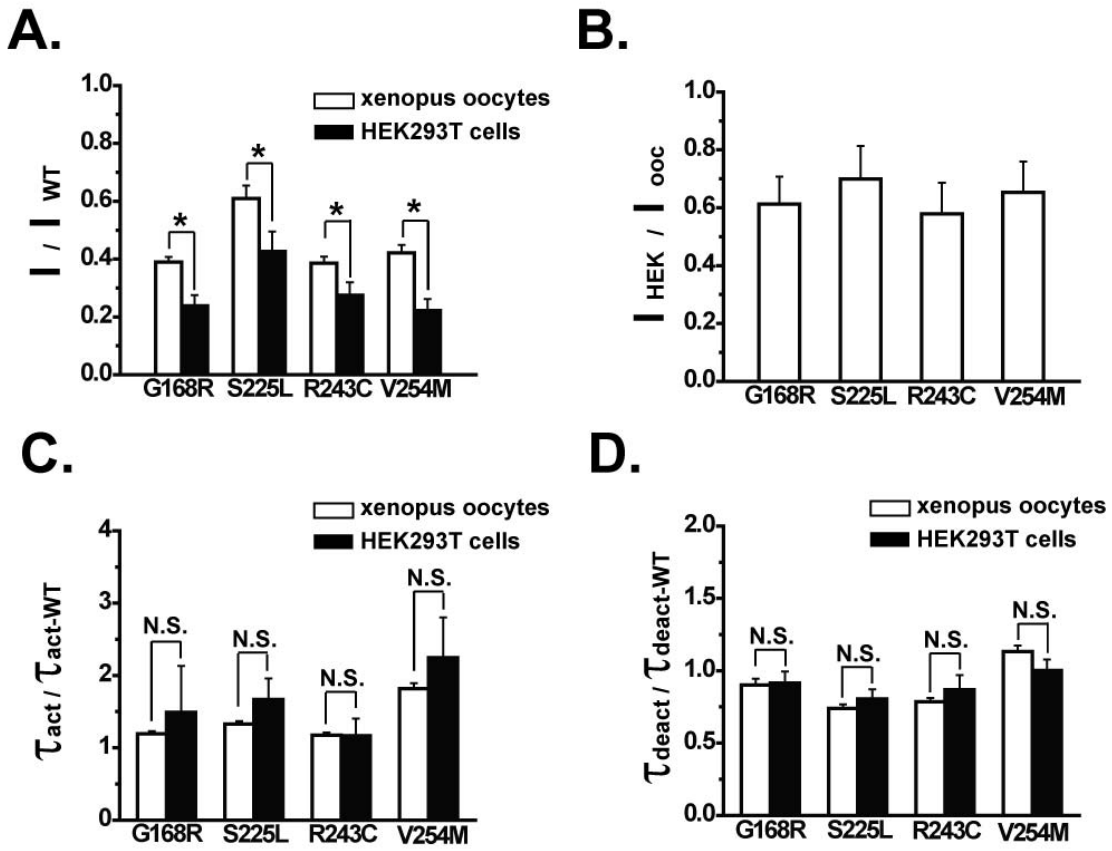
A.
B.
C.
D.
xenopus oocytes
HEK293T cells
I / I WT
I HEK / I ooc
τact / τact-WT
τdeact / τdeact-WT
G168R
S225L
R243C
V254M
*
N.S.

Fig. S2. Changes in ion channel parameters observed in LQT1-mutant channels expressed in mammalian system. Mutant channel subunits are expressed together with wild type subunits and the auxiliary KCNE1 subunits at a ratio 0.5 Q1WT: 0.5 Q1mut: 1.0 E1 in HEK293T cells. Values are normalized by the values measured in the channels that mimic the haploinsufficient phenotype (0.5 WT) (n=40). **A:** Comparison of I / I_{WT} observed in HEK293T cells (black bars) (G168R: N=18, S225L: N=16, R243C: N=14, V254M: N=13) and in *Xenopus* oocytes (white bars) (see Table 2). * $p < 0.05$. **B:** Proportions between I / I_{WT} in HEK293T cells (I_{HEK}) and that in *Xenopus* oocytes (I_{ooc}). There is no significant difference between any mutant channels. **C:** Comparison of $\tau_{act} / \tau_{act\text{-}WT}$ observed in HEK293T cells (black bars) and in *Xenopus* oocytes (see Table 2). N. S. shows "no significant difference". . **C:** Comparison of $\tau_{deact} / \tau_{deact\text{-}WT}$ observed in HEK293T cells (black bars) and in *Xenopus* oocytes (black bars) (see Table 2). N. S. shows "no significant difference".

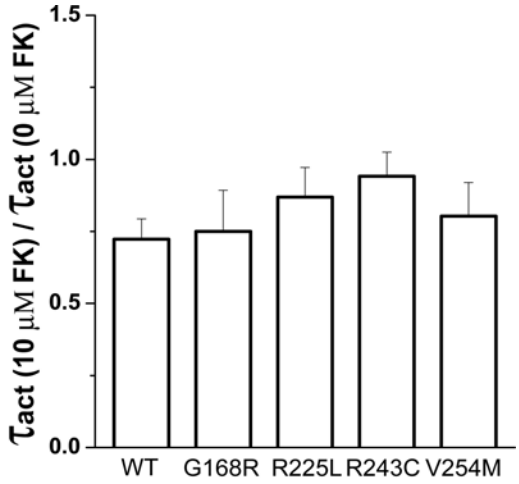

Fig. S3. Effect of PKA activation on channel activation kinetics in LQT1-mutant channels expressed in mammalian system. Mutant channel subunits are expressed together with wild type subunits and the auxiliary KCNE1 subunits at a ratio 0.5 Q1WT: 0.5 Q1mut: 1.0 E1 in HEK293T cells. Cells were stimulated by PKA activator forskolin (10 μM) for 10min and τ_{act} changes was measured from the same cell before and after stimulation. Currents were activated by 2-sec depolarization pulse to +20 mV from -80 mV holding potential. Ratios of τ_{act} before and after forskolin stimulation were shown in bar graphs (WT:N=12, G168R: N=7, S225L: N=6, R243C: N=9, V254M: N=6). No significant differences were observed between WT and mutants channel regarding the effect of PKA activation on τ_{act} (G168R: P=0.9991, S225L: P=0.7197, R243C: P=0.2681, V254M: P=0.9535 compared to WT).

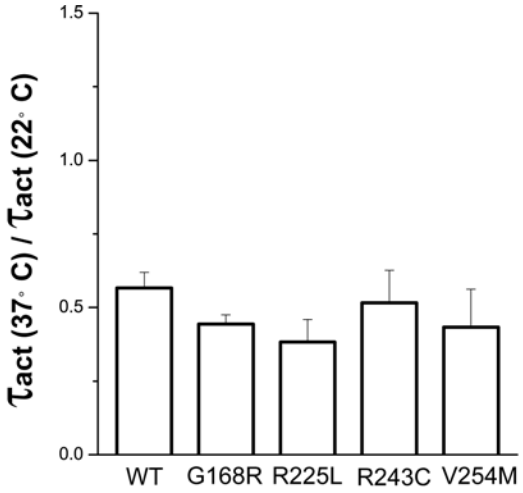

Fig. S4. Effect of temperature on channel activation kinetics in LQT1-mutant channels expressed in mammalian cells. Mutant channel subunits are expressed together with wild type subunits and the auxiliary KCNE1 subunits at a ratio 0.5 Q1WT: 0.5 Q1mut: 1.0 E1 in HEK293T cells. Cells were first perfused with extracellular solution at room temperature (22°C) and the perfusion solution was switched to 37°C for 3min. τ_{act} was measured from same cell at 22°C and 37°C. Currents were activated by 2-sec depolarization pulse to +20 mV from -80 mV holding potential. Ratios of τ_{act} at 22°C and 37°C were shown in bar graphs (WT:N=12, G168R: N=7, S225L: N=6, R243C: N=9, V254M: N=6). No significant differences were observed between WT and mutants channel temperature dependent effect on τ_{act} (G168R: P=0.9991, S225L: P=0.7197, R243C: P=0.2681, V254M: P=0.9535 compared to WT).

Table S1. Changes in voltage dependence parameters for channels expressing LQT1 mutant subunits. Changes in parameters obtained from Boltzmann equation fit of the channel tail current measured at -40 mV after a series of depolarizing voltages from -50 mV to +80 mV.

	$\Delta V_{1/2}$			k/k-WT			Gmax/Gmax-WT		
Mutation	**n**	**mean**	**SE**	**n**	**mean**	**SE**	**n**	**mean**	**SE**
WT	56	0.69	±0.77	56	0.99	±0.02	56	1.20*	±0.05
WT 0.5	97	0.00	±0.45	97	1.00	±0.01	97	1.00	±0.03
G168R	23	3.94	±0.89	23	1.00	±0.03	23	0.50*	±0.04
Y184S	18	2.91	±0.93	18	1.02	±0.02	18	0.82	±0.07
S225L	24	10.20*	±0.86	24	1.02	±0.02	24	0.87	±0.06
R243C	36	7.43*	±0.81	36	1.04	±0.81	36	0.61*	±0.04
V254M	25	24.00*	±1.31	25	1.09	±0.02	25	0.91	±0.07
L266P	24	4.44*	±1.60	24	1.00	±0.02	24	0.39*	±0.05
G269S	27	7.32*	±0.79	27	1.05	±0.03	27	0.66*	±0.06
W305S	34	5.25*	±1.16	34	0.93	±0.03	34	0.59*	±0.06
T312I	20	4.09	±0.89	20	0.84*	±0.04	20	0.40*	±0.06
G314S	19	3.55	±1.69	19	1.02	±0.09	19	0.31*	±0.03
Y315C	24	-0.72	±0.81	24	0.99	±0.03	24	0.60*	±0.04
A341E	28	3.79*	±1.17	28	1.05	±0.05	28	0.60*	±0.05
A341V	25	2.47	±0.83	25	0.96	±0.03	25	1.01	±0.12
S349W	30	18.97*	±1.54	30	1.26*	±0.02	30	1.50*	±0.07
R591H	25	0.23	±0.91	25	1.03	±0.02	25	1.12	±0.07
R594Q	26	1.52	±0.73	26	1.04	±0.03	26	0.98	±0.06

D611Y	27	0.80	±0.92	27	1.04	±0.03	27	1.35*	±0.09

Table S2. Results from simple linear regression.

Simple linear regression between the observed median QTc and the observed 30-year Kaplan Meier event free survival rates and the shift in $V_{1/2}$ and changes in Gmax caused by expression of mutant subunits.

Variable	Median QTc		30 year survival rate	
	adjR^2	p	adjR^2	p
$\Delta V_{1/2}$	0.05	0.19	0.074	0.14
Gmax/Gmax-WT	0.28	0.023	0.023	0.54

Reference List

1. Matavel, A. & Lopes, C. M. B. (2009) *Journal of Molecular and Cellular Cardiology* **46**, 704-712.

2. Matavel, A., Medei, E., & Lopes, C. M. (2010) *Channels (Austin.)* **4**, 3-11.

3. Bianchi, L., Priori, S. G., Napolitano, C., Surewicz, K. A., Dennis, A. T., Memmi, M., Schwartz, P. J., & Brown, A. M. (2000) *Am. J. Physiol Heart Circ. Physiol* **279**, H3003-H3011.

4. Flaim, S. N., Giles, W. R., & McCulloch, A. D. (2007) *Heart Rhythm* **4**, 768-778.

5. Reumann, M., Gurev, V., & Rice, J. J. (2009) *Personalized Medicine* **6**, 45-66.

6. Wettwer, E., Amos, G., Gath, J., Zerkowski, H. R., Reidemeister, J. C., & Ravens, U. (1993) *Cardiovasc. Res.* **27**, 1662-1669.

7. Li, G. R., Feng, J., Wang, Z., Fermini, B., & Nattel, S. (1995) *Am. J. Physiol* **269**, H463-H472.

8. Imredy, J. P., Penniman, J. R., Dech, S. J., Irving, W. D., & Salata, J. J. (2008) *American Journal of Physiology-Heart and Circulatory Physiology* **295**, H1867-H1881.

9. Li, G. R., Feng, J., Yue, L., Carrier, M., & Nattel, S. (1996) *Circ. Res.* **78**, 689-696.

10. Schwartz PJ, Priori SG, Spazzolini C, Moss AJ, Vincent GM, Napolitano C, Denjoy I, Guicheney P, Breithardt G, Keating MT *et al.* (2001) *Circulation* **103**, 89-95.

11. Walsh KB & Kass RS (1988) *Science* **242**, 67-69.

12. Findlay, I., Suzuki, S., Murakami, S., & Kurachi, Y. (2008) *Progress in Biophysics & Molecular Biology* **96**, 482-498.

13. Morimoto, S., Uchi, J., Kawai, M., Hoshina, T., Kusakari, Y., Komukai, K., Sasaki, H., Hongo, K., & Kurihara, S. (2009) *Biochem. Biophys. Res. Commun.* **390**, 87-92.

14. Yue, D. T., Herzig, S., & Marban, E. (1990) *Proc. Natl. Acad. Sci. U. S. A* **87**, 753-757.

15. Findlay, I. (2002) *Journal of Physiology-London* **541**, 741-751.

16. Findlay, I. (2004) *Journal of Physiology-London* **554**, 275-283.

Au: Please combine these materials and methods with those in the main paper, streamline them and move all to main paper.
Au: Please remove all place names from the materials and methods.